Direct double photoionization of atomic sodium

B. Rouvellou, L. Journel, J. M. Bizau, D. Cubaynes, and F. J. Wuilleumier
Laboratoire de Spectroscopie Atomique et Ionique, Unité de Recherche Associée au CNRS (URA 775), Bâtiment 350, Université Paris-Sud, F-91405 Orsay, France

M. Richter, K.-H. Selbmann, P. Sladeczek, and P. Zimmermann
Institut für Strahlungs -und Kernphysik, Technische Universität Berlin, Hardenbergstraße 36, D 10623 Berlin, Germany
(Received 15 April 1994)

Double photoionization of atomic Na has been investigated by combining the results of photoelectron and photoion spectroscopies from synchrotron radiation measurements in the photon energy range between 50 and 135 eV. Distinction with regard to the double-photoionization mechanism (one-step or two-step processes) and to final-state configuration allowed an accurate determination of the relative cross section for one-step direct double photoionization. Above 71 eV photon energy double photoionization is dominated by 2*s* photoionization followed by Auger decay (two-step process) whereas direct double photoionization accounts for only $\cong 20\%$ of double photoionization.

PACS number(s): 32.80.Hd, 32.80.Fb

I. INTRODUCTION

Double photoionization in the outer shell of an atom is a process of particular theoretical interest because it must be interpreted as a pure many-electron effect [1]. The relative intensity of direct double photoionization as compared to the total photoionization strength can be regarded as a measure of electron correlation within the atomic subshells. In particular, the threshold behavior of the double-photoionization cross section is considered to be of special importance, since the fundamental work by Wannier [2]. Direct double photoionization is often called shakeoff. This designation will not be used in the following part of this paper, because it is somewhat confusing. In the many-body diagrams describing double photoionization, the diagram actually corresponding to shakeoff, i.e., to core relaxation, is only one among others.

After the early work of Carlson [3] using laboratory x-ray sources, several experiments using radiation emitted by the first synchrotron radiation sources have measured the energy dependence of the branching ratio between double- and single-photoionization cross sections in the outer shell of the rare gases [4,5] and of some atomic vapors [6–9]. They found that double photoionization sometimes contributes significantly to the total photoabsorption cross section, and provides the material for a critical test of atomic calculations. Many-body perturbation theory was used at that time to calculate double-photoionization cross sections [1,10]. Agreement with the first experimental data available was reasonably good for the simplest rare gases, in particular for helium [11].

Over the past ten years the study of double-photoionization processes in atomic *outer* shells has been developed extensively [12–27] owing to the dramatic improvements achieved in the intensity of monochromatic beams of synchrotron radiation (SR) available with newly built dedicated storage rings. In particular, special attention was paid to the threshold [15–23] and high-energy [24–27] behavior of the double-photoionization cross section. Particular emphasis was put on helium, which is still the favorite candidate for such studies, because it provides the simplest model system to investigate the breakup of a three-body system into two free electrons and a positive ion. The energy dependence of the branching ratio $\sigma(\mathrm{He})^{2+}/\sigma(\mathrm{He})^{+}$ was carefully measured in a number of accurate experiments [24–27], up to very high photon energies (12 keV). Double and triple photoionization in oxygen [28] and nitrogen [29] were also studied to determine the threshold behavior of the cross sections for the yield of doubly and triply charged ions. Using coincidence experimental setups, the relative intensities for production of different final states of doubly charged ions have been measured in neon and argon [20,22,23]. More recently, the energy distribution of both electrons emitted in the double-photoionization process has been measured at various excess energies above the double-photoionization threshold in helium [19]. The results of these measurements confirm the prediction of an early calculation made in the case of double photoionization in the outer 2*p* subshell of neon, using many-body perturbation theory [1]. At high excess energy above the double-photoionization threshold, the intensity of low and fast electrons is strongly enhanced, producing a characteristic U-shape distribution. When approaching the double-ionization threshold, this distribution turns out to be flat. Ultimately, some results have been obtained in the study of energy- and angle-resolved double photoionization, measuring coincidences between both electrons ejected in the double-photoionization processes in krypton and in xenon [30–33] using the He II line as the source of photons, and in helium [34,35] using synchrotron radiation. Following this intense experimental activity, considerable progress has also been made in the theoretical description of the process, in particular for helium [36–41].

When a vacancy occurs in the *inner* shell of an atom by

photoabsorption of a single photon, doubly charged ions can be produced as the result of two different mechanisms. In the one-step double-photoionization process, a second electron can be ejected simultaneously from the outer shell, again via correlation effects [1]. In the two-step process [13–15,42], the ejection of the first electron is followed by Auger decay of the singly charged ion, producing, in the simplest case, doubly charged ions. Double Auger decay can also occur, the excess energy being distributed between two electrons that are simultaneously ejected from the singly charged ion, leading to triply charged ions. Experimental evidence for direct double-photoionization processes [43] and for double Auger decay [44,45] was found many years ago.

Since 1984, a large number of experimental studies have been performed, dealing mostly with multiple photoionization following inner-shell photoexcitation or ionization in the rare gases [46–60] and in some atomic vapors [61–71]. Electron and mass specrometries have both been used. In a photoelectron spectrum, a one-step double-photoionization process shows up as a continuum without any discrete structure, because the energy available is shared continuously between the two ejected electrons, and a two-step double photoionization process is identified by the observation of discrete Auger lines corresponding to the ejection of electrons with characteristic energy in each step. In addition, it is possible to discriminate electrons ejected in direct double photoionization from electrons emitted in the double Auger processes, because of their different energy distribution. In an ion spectrum, both one- and two-step process produce doubly charged ions Thus it is usually not possible to distinguish between one- and two-step processes in measuring only the relative abundance of singly and doubly charged ions.

When double photoionization occurs as the consequence of the excitation of an inner electron onto an excited orbital, the analysis is made more complicated because the excited electron can act either as an actor or as a spectator in the relaxation of the core-excited state [72]. When it behaves as an actor, it can be shaken up to a higher excited orbital or shaken off into the double-photoionization continuum in the so-called resonant double Auger process. The competition between these two categories of transitions has been qualitatively observed and quantitatively measured in the rare gases, using both electron and ion spectrometries [53,55,58,72]. The latest results obtained for the rare gases [53,55] establish that shake-up processes gain in intensity with increasing quantum numbers of the excited electron orbital, and that the most important route to doubly charged ions is via a two-step Auger decay. Since the one-step direct double-photoionization cross section was found to be negligible as compared to the resonant double-photoionization cross section, no interference effect has been observed, and only Lorentzian profiles have been measured in the double-photoionization channel [53]. Direct evidence has been found recently for such an interference effect from the observation of a Fano profile in the double-photoionization continuum of core-excited sodium atoms [73], as will be briefly explained in Sec. II of this paper.

II. DIRECT DOUBLE PHOTOIONIZATION INVOLVING ELECTRONS OF TWO DIFFERENT SUBSHELLS: THE SODIUM CASE

Alkali-metal atoms are unique candidates to study multiple-ionization processes following inner-shell excitation or ionization, because of their specific electronic structure, with only one outer electron outside of a closed core. Among them, sodium has been extensively studied during the past few years. For several specific reasons, atomic sodium in the $1s^2 2s^2 2p^6 3s$ ground state has been chosen and investigated.

(a) The energy-level diagrams Na, Na^+, and Na^{2+} are schematically shown in Fig. 1. Single photoionization of neutral sodium in the $3s$, $2p$, and $2s$ subshells requires 5.14, 38.0, and 71.0 eV, respectively. The first double-ionization threshold [74], involving simultaneous removal of the outer shell $3s$ and first inner-shell $2p$ electrons, occurs at 52.4 eV, according to

$$\mathrm{Na}:2s^2 2p^6 3s\ {}^2S + h\nu \rightarrow \mathrm{Na}^{2+}:2s^2 2p^5\ {}^2P + \varepsilon l + \varepsilon' l' \ . \qquad (1)$$

This means that, between 52.4- and 71.0-eV energy, the two-step Auger route cannot occur. Thus only one-step double photoionization involving the simultaneous ionization of a $2p$ inner electron and of the outer electron can produce doubly charged ions in this energy range.

(b) In the energy range above the $2s$ photoionization threshold, Na^{2+} ions can be formed by a one-step (direct double-photoionization process) as well as two-step process via $2s$ single photoionization followed by Auger decay, and the relative strengths of these different double-

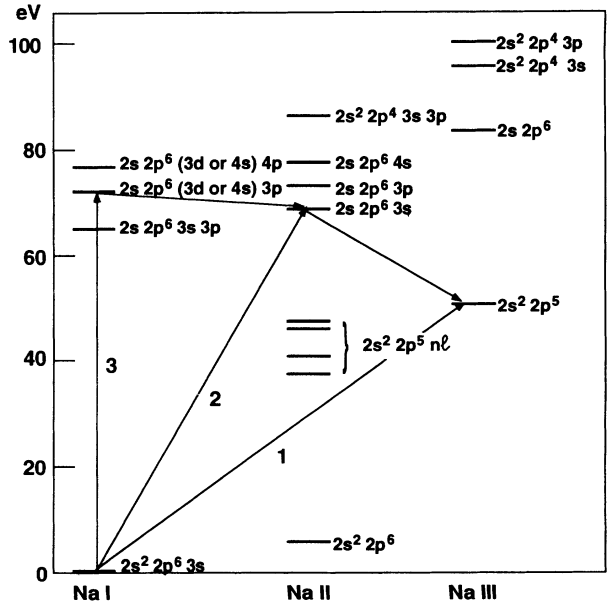

FIG. 1. Energy-level diagram of Na, Na^+, and Na^{2+}. The energy scale refers to the ground state of neutral sodium. The three different double-ionization mechanisms discussed in the text (1, 2, and 3) are indicated in the figure. Energy levels are taken from Refs. [74] and [82].

photoionization mechanism can be compared, combining electron and ion spectrometries.

(c) Below 85.2-eV photon energy (energy of the second $2s2p^6\,^2S$ double-ionization threshold), only one Na^{2+} final-state configuration ($2s^22p^5$) can be reached, and a further distinction with regard to final-state configurations is not necessary. This implies that only one direct double-photoionization channel here contributes, which simplifies evaluation and interpretation of the data.

(d) At 66.6 eV and above, there are discrete core-excited states [75] forming Rydberg series converging to the $2s$ ionization thresholds ($2s2p^63s\,^1S$ at 71.0 eV and ^3S at 71.3 eV). These autoionization states are accessible by photoexcitation of a $2s$ electron according to

$$\mathrm{Na}{:}2s^22p^63s\,^2S+h\nu\rightarrow\mathrm{Na}^*{:}2s2p^63snp\,^2P\ . \qquad (2)$$

Earlier photoabsorption measurements [75,76] observed and identified the first members of the series. These excited states lie above the first $2s^22p^5\,^2P_{1/2,3/2}$ double-ionization thresholds, but below the next inner-shell single-ionization and the second double-ionization ($2s^22p^5$, at 85.2 eV) thresholds. At 66.6 eV, the excited $2s2p^63s(^3S)3p\,^2P$ state decays preferentially by autoionization. One of the possible decay routes is to the $2s^22p^5\,^2P$ doubly ionized states. At this photon energy, the direct one-step double photoionization can interfere on resonance with the resonant double Auger process (also called resonant double autoionization). All other relaxation schemes lead to singly charged final states of Na^+ ions [73].

(e) Direct $2p$-subshell photoionization into the continuum leaves the core-ionized ion in its state of lowest energy, $2s^22p^53s\,^{1,3}P$, with only one $2p$ electron being removed (corresponding to the so-called main line in a photoelectron spectrum), according to

$$\mathrm{Na}{:}2s^22p^63s\,^2S_{1/2}+h\nu\rightarrow\mathrm{Na}^+{:}2s^22p^53s\,^{1,3}P_{1/2,3/2}+\varepsilon l\ , \qquad (3)$$

or, in a higher excited sate, corresponding to the correlation satellite lines: (i) $2s^22p^53p\,^{1,3}L_{1/2,3/2}$ and $2s^22p^54p\,^{1,3}L_{1/2,3/2}$ states, with the outer $3s$ electron being simultaneously excited onto a $3p$ or $4p$ orbital via continuum state interaction (the excited electron has changed its orbital quantum number by one unit), according to

$$\mathrm{Na}{:}2s^22p^63s\,^2S_{1/2}+h\nu\rightarrow\mathrm{Na}^+{:}2s^22p^5np\,^{1,3}L_{1/2,3/2}+\varepsilon l\ , \qquad (4)$$

giving rise to what has been called the "conjugate shake-up" satellites (CSU); (ii) $2s^22p^54s\,^{1,3}P$ and $2s^22p^55s\,^{1,3}P$ states, with the $3s$ outer electron being simultaneously excited onto a $4s$ or $5s$ orbital via a monopole transition (the excited electron does not change its orbital quantum number), according to, e.g.,

$$\mathrm{Na}{:}2s^22p^63s\,^2S_{1/2}+h\nu\rightarrow\mathrm{Na}^+{:}2s^22p^5ns\,^{1,3}P_{1/2,3/2}+\varepsilon l\ , \qquad (5)$$

producing the shake-up (SU) satellites, or onto a $3d$ orbital via second-order correlation effects. In previous work [77,78], the study of photoelectron spectra of sodium has demonstrated that the relative intensity of the SU and CSU satellites accompanying photoionization in the $2p$ subshell was high, about 20% and 10% when referred to the intensity of single photoionization, respectively. Since the relative intensities of correlation satellites and double photoionization, respectively, are roughly comparable, within a factor of 3, in photoionization of the outer shell of neon [4,79], the adjacent rare gas, it was important to determine if this behavior was also true when the double-photoionization process involves two different subshells. Such a comparison would give valuable information about the relative importance of the different correlation effects. Similar processes also occur following photoionization into the $2s$ subshell.

(f) From the theoretical point of view, sodium is an ideal case for testing the intensity of the direct double-photoionization process involving electrons from two different subshells, since there is only one electron outside of a closed electronic core. Then, in the many-body theory, the contribution of the various diagrams describing the various interactions leading to a doubly charged ions, i.e., mainly core relaxation, inelastic scattering, and ground-state correlations, can be more easily disentangled. Progress in this way has recently been made [80].

III. EXPERIMENT

In the work presented here, we have measured the relative abundance of Na^+ and Na^{2+} ions produced between 52.4- and 135-eV photon energy, and we have combined these results with some additional data we have recently obtained using electron spectroscopy.

Synchrotron radiation from the BESSY storage ring was used between 50 and 135 eV to analyze the ratio of Na^{2+} to Na^+ ions produced by photoionization. A schematic view of the experimental setup is shown in Fig. 2. The light emitted from a bending magnet of BESSY was monochromatized by a toroidal grating monochromator (TGM) with a resolution $h\nu/\Delta h\nu=250$. Using a 950 lines/mm grating, the photon flux was $\cong 4\times10^{10}$ photons/sec in a band pass of 0.3 eV at 65-eV photon en-

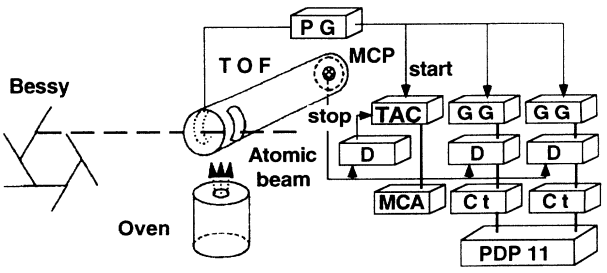

FIG. 2. Scheme of the experimental setup used for photoion spectrometry as described in the text. TOF, time-of-flight ion tube; PG, pulse generator; MCP, multiarray channel plate; TAC, time-to-amplitude converter; GG, gate generator; *D*, discriminator; *Ct*, counter; MCA, multichannel analyzer.

ergy, and for 100-mA electron current in the ring. To suppress higher-order contributions to the monochromatized light below 72 eV, we mounted an aluminum foil of 1000-Å thickness into the beam. The monochromatized light was focused into the interaction zone of a time-of-flight (TOF) ion-mass analyzer, where it crossed a beam of Na atoms generated by a resistively heated furnace. Ions produced by photoionization were extracted and accelerated into the drift section of the TOF by electrostatic pulses of 100-V amplitude, a pulse length of typically 2 μs, and a pulse frequency of 25 kHz. Measuring the time of flight of the ions between interaction zone and detector, a separation with regard to the ratio of mass and charge was possible.

Synchrotron radiation from the Super ACO storage ring in the photon energy range between 70 and 125 eV was used to obtain series of photoelectron spectra of atomic sodium. The light was monochromatized by a TGM ($h\nu/\Delta h\nu$ ranging from 100 up to 250) and focused into the interaction zone of a cylindrical-mirror electron analyzer where it crossed a beam of Na atoms. Electrons produced by photoionization were analyzed with an energy resolution power of $\cong 100$. Accepting the electrons emitted under the main angle θ of 54.7° to the direction of the synchrotron radiation beam allows to suppress any angular distribution effects in the electron signal, provided the cylindrical-mirror analyzer (CMA) axis is colinear to the direction of the SR. It has been demonstrated [77] that, for an isotropic initial state, the signal produced by electrons ejected at this angle is independent of the elliptical polarization of the radiation, since integration in the $(0,2\pi)$ angular range over the ϕ angle between the direction of propagation of the photoelectrons and polarization axes of SR cancels any ϕ dependence. Under these conditions, the electron signal detected by the channeltron located on the axis of the CMA is strictly proportional to the absolute cross section (in the dipole approximation valid here). A detailed description of the experimental setup and procedure can be found elsewhere [78]. Relative intensities could be deduced for all important photoionization process in this energy range, including a qualitative estimation of the double-photoionization intensity at 116-eV photon energy.

Two examples of TOF ion spectra, one measured at 80-eV photon energy, the other one at 132 eV, are shown in Fig. 3, in the upper and lower parts, respectively. Numerous ionic lines appear, partly due to photoionization of the residual molecular gases by synchrotron radiation. At 80-eV photon energy, i.e., a few eV above the $2s$ ionization threshold, the most intense signal is the Na^+ ion line around channel number 2500. Near channel number 1700, one observes also a very small signal that can be identified as a Na^{2+} ion line produced by one- and two-step double photoionization of Na atoms. At 132-eV photon energy, the relative intensity of the ion line measuring the quantity of Na^{2+} doubly charged ions has increased significantly, as compared to the Na^+ ion signal, because more channels are open into the double-ionization continuum, reflecting an increase of the relative double-photoionization cross section. For a large

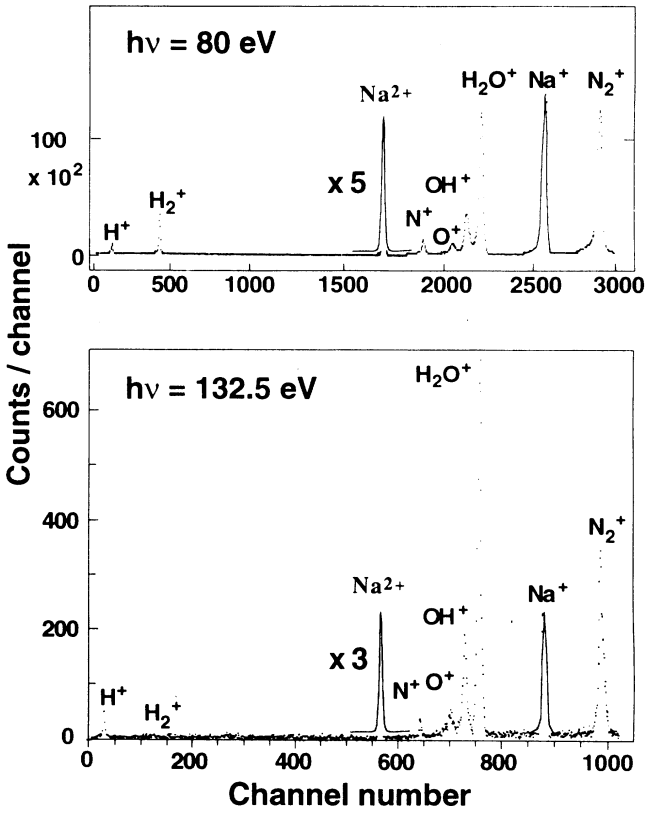

FIG. 3. Two time-of-flight (TOF) ion spectra measured at 80- (upper part) and 132-eV (lower part) photon energies. Ionic lines due to single and double photoionization of atomic sodium are marked by multiplicative factor.

number of photon energies, the ratio of Na^{2+} and Na^+ intensities was measured from spectra similar to the ones shown in Fig. 3. A significant Na^{3+} signal expected only above 124-eV photon energy [74] was not detected in the energy range up to 135 eV.

An example of a photoelectron spectrum, taken at 116-eV photon energy, is shown in Fig. 4. The photoelectron lines between 63.6- and 77-eV kinetic energy correspond to photoionization of the $2p$ subshell, which is dominated by the single-photoionization process, according to (3), at 38-eV binding energy, accompanied by correlation satellites, processes (4) and (5), between 42- and 60-eV binding energy. Besides the weak $3s$ photoionization, these are the processes which form a Na^+ ion in the final state. The series of $2s^22p^5nl\varepsilon'l'$ satellites converges toward the threshold for $2s^22p^5\varepsilon l\varepsilon'l'$ double photoionization. In the spectrum of Fig. 4, this threshold is located at 63.6-eV kinetic energy, and the double-photoionization continuum manifests itself as an unstructured background between 0- and 63.6-eV kinetic energy (hatched and black areas in the figure). At low electron kinetic energies, i.e., below 5-eV kinetic energy, the transmission of the CMA is poor, which explains why we do not observe the enhancement of the low-energy part of the U-shape distribution.

The photoelectron lines between 31- and 44-eV kinetic

energy correspond to photoionization of the $2s$ shell, which again is dominated by the single photoionization of a $2s$ electron at 71-eV binding energy ($2s2p^6 3s\ ^{1,3}S$ final ionic states), accompanied by correlation satellites between 75- and 85-eV binding energy ($2s2p^6 nl\ ^{1,3}L$). As mentioned above a vacancy produced in the $2s$ subshell is able to decay by an Auger process into the Na^{2+} ground state, according to

$$Na^+:1s^2 2s 2p^6 n'l' \rightarrow Na^{2+}:1s^2 2s^2 2p^5 + (\varepsilon l)_{\text{Auger}} . \quad (6)$$

The corresponding Auger lines arise between 18- and 30-eV kinetic energy as a direct mirror image of the $2s$ photolines, overlapped by molecular emission [81,82]. Correlation satellite lines due to transitions

$$Na:1s^2 2s^2 2p^6 3s + h\nu \rightarrow Na^+:1s^2 2s^2 2p^4 3s 3p + \varepsilon l , \quad (7)$$

are located between 20- and 30-eV kinetic energy. At 116 eV, they overlap with the $2s2p^6 n'l' \rightarrow 2s^2 2p^5 + (\varepsilon l)_{\text{Auger}}$ Auger lines, as do the corresponding $2s^2 2p^4 3s 3p \rightarrow 2s^2 2p^5 + (\varepsilon l)_{\text{Auger}}$ Auger lines with the $2s2p^6 n'l'$ photolines. However, these latter processes are responsible for a Na^{2+} ion in the final state reached by a two-step process. Their relative strength was obtained by a number of photoelectron spectra taken at different photon energies.

Finally, the residual background blackened in Fig. 4 between 32- and 64-eV kinetic energy after background subtraction corresponds to the high-energy part of the continuous energy distribution of the two outgoing electrons emitted in double photoionization of sodium by 116-eV photons, i.e., to the high-energy half of the U-shape distribution predicted by Chang and Poe [1]. It is interesting to note that the shape of this continuous distribution does not show any apparent change at the $2s2p^6$ Na^{2+} double-ionization threshold (85.2-eV binding energy). This observation demonstrates that double photoionization into the $2s2p^6$ continuum of the Na^{2+} ion is weak compared to the $2s^2 2p^5$ continuum. An electron spectrum such as the one shown in Fig. 4 illustrates the potentiality of electron spectroscopy to discriminate against the different electrons ejected in various double-photoionization continua. Thus one can estimate that the integral intensity of the continuous distribution in the 31.8–63.6-eV kinetic-energy region (blackened area in Fig. 4) is equal to the value of the $(2p,3s)$ double-ionization cross section. Since all features due to single ionization are also observed in the spectrum, it is possible to evaluate the double-to-single photoionization ratio. The result is about 3% within some large error bars, because it is difficult to correct with accuracy for the background due to other sources. Thus, although this number cannot be considered a quantitative measurement of the relative intensity of the direct double-photoionization process, it suggested that the direct double-photoionization process producing simultaneous ejection of one $2p$ electron and one $3s$ electron has a relative intensity smaller by far than the relative intensity (more than 30%) of the correlation satellites involving electrons from the same subshells.

After proper instrumental corrections, mainly for the ion detector efficiency, have been applied to the data measured by photoion spectrometry, the total (one- and two-step processes) relative cross section for formation of Na^{2+} ions was obtained as a function of photon energy.

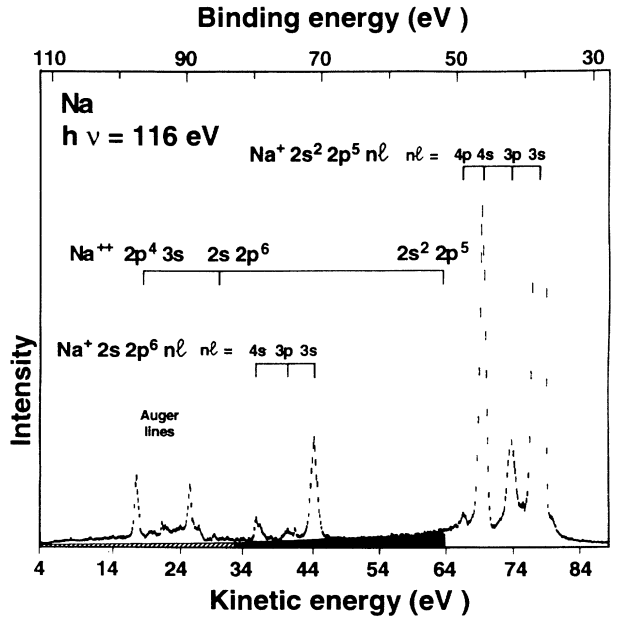

FIG. 4. Photoelectron spectrum of atomic Na taken at 116-eV photon energy. The half-high-energy part of the electron distribution due to direct double photoionization is indicated in black between 64- and 32-eV kinetic energies, the half-low-energy part is shown as hatched area. The strength of the $2s^2 2p^5 3s$ main line (single $2p$ photoionization) at ~38-eV binding energy exceeds the range of the y axis.

IV. RESULTS AND DISCUSSION

Figure 5 shows the relative cross section for double photoionization of atomic Na as a function of photon energy. The overall accuracy on these measurements is ±5%, except very near threshold, where the double-photoionization cross section is very low, starting from a zero value at threshold. As expected, below 52.4 eV, which is the first threshold for double photoionization [74], no Na^{2+} signal is observed. Between 52.4 and 71.0 eV only direct double photoionization of Na atoms, according to (1), contributes to the formation of Na^{2+} ions, since the other open channels following inner-shell photoionization, i.e., production of a single hole in the $2p$ subshell, with possible excitation of the $3s$ outer electron, do not allow any following Auger decay and end up in Na^+ states [74]. Therefore the cross section between 52.4 and 71.0 eV for $(2p,3s)$ direct double-photoionization processes into the $2s^2 2p^5 \varepsilon l \varepsilon' l'$ continuum can be read off directly from Fig. 5 to increase from 0 to ~1% of the total photoionization cross section. The Fano-type structure at ~66.6 eV indicates coupling of the double-photoionization process to the corresponding $2s \rightarrow 3p$ resonance of Na via the sequence

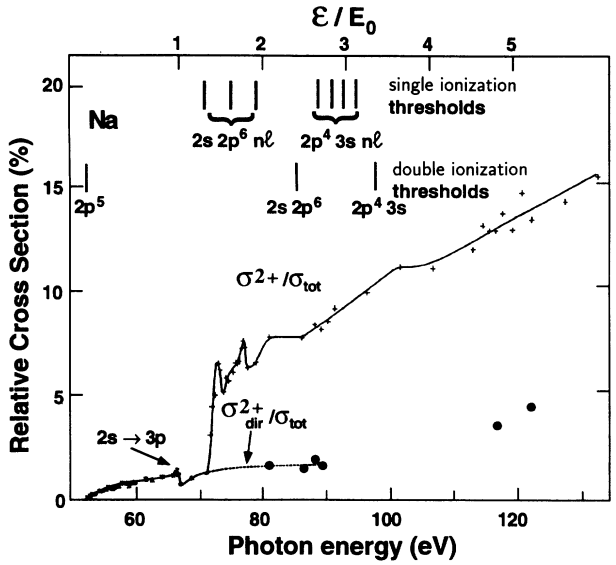

FIG. 5. Variation, as a function of photon energy, of the double-photoionization cross section (+++, above 71 eV) and the direct double-photoionization cross section (*xxx*, below 71 eV). The black circles are the values of the direct double photoionization cross section above 71 and 110 eV, respectively. They have been determined as explained in the text. All data are normalized to the total photoionization cross section. The thresholds for single and double ionization are indicated by vertical bars [65].

$$\begin{aligned}&\mathrm{Na}:2s^2 2p^6 3s\ {}^2S_{1/2}+h\nu\\&\quad\rightarrow \mathrm{Na}^*:2s2p^6 3s3p\ {}^2P_{1/2,3/2}\\&\quad\rightarrow \mathrm{Na}^{2+}:2s^2 2p^5\,{}^2P_{1/2,3/2}+\varepsilon l+\varepsilon' l'\ .\end{aligned}\tag{8}$$

Details on this direct observation of a Fano profile into a double-photoionization continuum have already been published [73]. Here let us mention only that a recent R-matrix calculation [83] of the natural width Γ and profile index q of the $2s\rightarrow 3p$ resonance line in the total photoabsorption cross section gives a value of 0.24 eV and -1.81, respectively, in excellent agreement with the experimentally measured values (0.23 eV and -1.73) [73].

At 71.0-eV photon energy, photoionization of the $2s$ shell starts, now leading via Auger decay to the same Na^{2+} final ionic state, according to

$$\mathrm{Na}^+:2s2p^6 3s\rightarrow \mathrm{Na}^{2+}:2s^2 2p^5+\varepsilon l_{\mathrm{Auger}}\ ,\tag{9}$$

which is manifested by a sudden increase in the Na^{2+} signal. The experimental results are shown as crosses in the figure. Above 71 eV, there is a large number of additional thresholds for photoionization in the $2s$ and $2p$ subshells. The main ones are the $2s2p^6 nl$ series converging to the $2s2p^6$ direct double-ionization threshold at 85.2 eV ($2s2p^6\varepsilon l\varepsilon' l'$ final states) and the $2s^2 2p^4 nln' l'$ series beginning at about 90 eV and converging to the $2s^2 2p^4 nl\varepsilon' l'\varepsilon'' l''$ double-ionization threshold at 97.8 eV. All these Na^+ singly charged ionic states decay to Na^{2+} doubly charged ion via Auger decay [6]. The opening of these satellite channels ending up in the Na^{2+} ground state also gives reason for the gradual increase of σ^{2+} with respect to σ_{tot} above 71 eV. These single-ionization thresholds and the different double-ionization thresholds are indicated in Fig. 5 by vertical bars [74,82].

Summarizing the situation, the ratio $\sigma^{2+}/\sigma_{\mathrm{tot}}$ was accurately measured by photoion spectroscopy and the ratio σ^{2+} (two-step)$/\sigma_{\mathrm{tot}}$ by photoelectron spectroscopy. Then, for photon energy values above 71 eV, the relative intensity of the direct double-photoionization process $\sigma^{2+}_{\mathrm{dir}}$ is obtained by

$$\sigma^{2+}_{\mathrm{dir}}/\sigma_{\mathrm{tot}}=\sigma^{2+}/\sigma_{\mathrm{tot}}-\sigma^{2+}_{\mathrm{two-step}}/\sigma_{\mathrm{tot}}\ ,$$

using photoelectron spectroscopy data whose a part was already published [68,69,74]. The values of the relative direct $(2p,3s)$ double-photoionization cross section (leaving the doubly charged ion into the $2s^2 2p^5\,{}^2P$ final ionic states) deduced in this way are shown in Fig. 5 as black circles below 90- and above 116-eV photon energy. The accuracy on these results is estimated to be $\pm 10\%$. Between 90 and 116 eV, overlaps between photoelectron and Auger lines prevent this determination from the experimental measurements.

The results show that this relative intensity seems to reach a plateau value of $\sim 1.5\%$ below 90-eV photon energy, whereas at ~ 120 eV the values obtained are higher ($\sim 3.5\%$, in close agreement with the estimation made from the spectrum shown in Fig. 4). These measurements confirm that direct $(2s,3s)$ double photoionization to the $2s2p^6$ final ionic states which starts at 85.2 eV does not make any important contribution, as was already clear from Fig. 4. Thus, up to 90-eV photon energy, our results are a measurement of the direct $(2p,3s)$ double-photoionization cross section ($2s^2 2p^5$ final ionic states). In Fig. 5, the upper energy scale shows the value of the reduced parameter ε/E_0 [79], where $\varepsilon=h\nu-E^*$ is the excess energy of the photon $h\nu$ over the energy necessary to produce double photoionization, i.e., to remove the $3s$ electron in the presence of the core hole in the $2p$ subshell. One notes that the plateau value for $(2p,3s)$ double photoionization is reached for low values of this reduced parameter, as was already measured for the probability of producing $2s^2 2p^5 nl$ correlation satellites [77,78]. In the adjacent rare gas neon, the plateau is reached for much higher values (10–12) [79] of the reduced parameter. This different behavior suggests that, in the case of double photoionization involving one inner electron and one outer electron, the most important correlation effects are core relaxation and inelastic scattering, while ground-state correlations play a role more important than core relaxation in explaining the intensity of double photoionization when both electrons belong to the same outer shell [3,4,79,85]. At higher photon energies, the large increase observed in the direct double-photoionization cross section is explained by the opening, at 97.8 eV, of the additional $(2p,2p)$ double-photoionization channel ($2s^2 2p^4 3s$ final ionic states), which obviously contributes significantly to the double-photoionization intensity.

Interesting details of the $\sigma^{2+}/\sigma_{\mathrm{tot}}$ curve in Fig. 5 are resonance structures at ~ 73- and ~ 77-eV photon energy which can be ascribed to

$$\mathrm{Na}:1s^2 2s^2 2p^6 3s + h\nu \rightarrow \mathrm{Na}^*:1s^2 2s 2p^6 3p 4s \quad (10)$$

and

$$\mathrm{Na}:1s^2 2s^2 2p^6 3s + h\nu \rightarrow \mathrm{Na}^*:1s^2 2s 2p^6 4s 4p \quad (11)$$

double excitations. They were also observed in absorption [84] and obviously coupled to Na^{2+} final states. The most probable route for that is a first Auger decay into the 2*s* continuum followed by a second one into the Na^{2+} final state, according to

$$\mathrm{Na}^*:1s^2 2s 2p^6 4s(3p,4p) \rightarrow \mathrm{Na}^+:1s^2 2s 2p^6 3s + (\varepsilon l)_{\mathrm{Auger}} \rightarrow \mathrm{Na}^{2+}:1s^2 2s^2 2p^5 + (\varepsilon' l')_{\mathrm{Auger}} . \quad (12)$$

This implies that the 2*s* inner hole is not affected by the first of these Auger processes, and remains as sort of "spectator," and decays only during the second one.

Going back to the energy level diagram in Fig. 1, we can illustrate this situation at these photon energies in the following way. Three different processes can contribute here at 73 or 77 eV to a Na^{2+} final state, as indicated in the figure by three arrows: (1) a one-step process, i.e., direct double photoionization ($\sim$20% at 73 eV); (2) a two-step process via 2*s* photoionization and Auger decay ($\sim$55% at 73 eV); and (3) a three-step process via double excitation and two-step Auger decay ($\sim$25% at 73 eV). The three-step process is resonant and only possible at fixed photon energies ($\sim$73 eV, $\sim$77 eV). The one- and two-step processes are nonresonant and therefore contribute the main part to the $\mathrm{Na} \rightarrow \mathrm{Na}^{2+}$ oscillator strength. Moreover, it is obvious that the two-step process via 2*s* photoionization and Auger decay dominates by far the Na^{2+} formation (55–80%).

Finally, in Table I we show a summary of the data comparing the relative intensity of correlation satellites and direct double-photoionization processes following photoionization in the 2*p* subshell of sodium (data presented here) with the values measured in the adjacent rare gas neon, photoionized in the 2*p* subshell [27,79,86-88]. The data are shown for the same values of the reduced parameter ε/E_0 [79], and refer to the total 2*p* photoionization cross sections. At 85-eV photon energy for the 2*p* subshell of sodium, i.e., below the second double-ionization threshold, $\varepsilon/E_0 = 2.35$. In neon, this parameter has the same value at about 160-eV photon energy, although this energy does not yet correspond to the plateau value of the probability of multiple-photoionization transitions. Whereas the total probability of multiple transitions (transitions producing correlation satellites and double photoionization) is roughly comparable in neon and sodium, the distribution of the oscillator strength between the two series of final-state channels is dramatically different in both cases. The relative intensity of the various correlation satellites and the double-photoionization process involving two electrons belonging to the same outer subshell are actually comparable in neon, although double photoionization is favored as compared to transitions producing correlation satellites. The double-photoionization channel involving the simultaneous ejection of one 2*p* electron and one 3*s* electron is very weak in sodium, with a plateau value of about 1%, as compared to the sum of the intensities of the various correlation satellites (more than 20%) at about the same relative excess photon energy above the threshold. An explanation of this different behavior in sodium can be found in the fact that, in single photoionization of the 3*s* electron, discrete excitations of the 3*s* electron to *np* orbitals take most of the oscillator strength, more than 0.8, and that such excitations of the 3*s* electron are still favored when they accompany inner-shell photoionization. Detailed calculations are in progress to check if theory is able to reproduce these results.

V. CONCLUSION

Data for direct double-photoionization strength involving inner-shell electrons are very rare in the literature, since in most of the publications absolute or relative

TABLE I. Branching ratios for 2*p* photoionization of Na (this work and Refs. [77] and [78]) and Ne (Refs. [27], [79], and [86–88]) into the various final-state channels at $\varepsilon/Eo = 2.35$ (85-eV photon energy in sodium, 160 eV in neon). The data are normalized to the total 2*p* photoionization cross section taken equal to 100.

	Na		Ne	
Process	Final-state configuration	Branching ratio	Final-state configuration	Branching ratio
2*p* single photoionization	$Na^+:2s^2 2p^5 3s\varepsilon l$	76	$Ne^+:2s^2 2p^5 \varepsilon l$	83
2*p* correlation satellites	$Na^{+*}:2s^2 2p^5 nl\varepsilon' l'$	23	$Ne^{+*}:2s^2 2p^4 nl\varepsilon' l'$	5
Double photoionization	$Na^{2+}:2s^2 2p^5 \varepsilon l\varepsilon' l'$	1	$Ne^{2+}:2s^2 2p^4 \varepsilon l\varepsilon' l'$	12
Correlation satellites/ double ionization		23		0.4

double-photoionization cross sections are given without any distinction with regard to the double-photoionization mechanism (one- or two-step process) or to the final-state configuration. Moreover, for a valuable test of the theoretical models taking into account electron correlations, the cross sections must be given on an absolute scale. For the present data the latter could be performed by using absolute absorption cross-section values [76] for σ_{tot} to calculate the cross section for direct double photoionization with the help of the measured ratio $\sigma_{\text{dir}}^{2+}/\sigma_{\text{tot}}$ in Fig. 5. At 85-eV photon energy, where only the $2s^2 2p^5 \varepsilon l \varepsilon' l'$ channel contributes, σ_{dir}^{2+} is found to account for ~ 0.12 Mb. This value is comparable to double-photoionization intensity in the outer shells of neon and argon, where np^6 subshells are also involved in the direct double-photoionization processes [4,27]. On the other hand, double photoionization of helium is more than ten times weaker in the same energy range [4,11,16,27]. For a deeper understanding of these results, many-body electron calculations are needed. Such calculations are in progress and will be presented elsewhere together with a complete experimental determination of the absolute partial-photoionization cross sections [89].

[1] T. N. Chang, T. Ishihara, and R. T. Poe, Phys. Rev. Lett. **27**, 838 (1971).

[2] G. H. Wannier, Phys. Rev. **90**, 817 (1953).

[3] T. A. Carlson, Phys. Rev. **156**, 142 (1967).

[4] V. Schmidt, N. Sandner, H. Kuntzemüller, P. Dhez, F. J. Wuilleumier, and E. Källne, Phys. Rev. A **13**, 1748 (1976).

[5] D. M. P. Holland, K. Codling, and G. V. Marr, J. Phys. B **12**, 2465 (1979).

[6] D. M. P. Holland and K. Codling, J. Phys. B **13**, L293 (1980); **13**, L745 (1980).

[7] D. M. P. Holland and K. Codling, J. Phys. B **14**, L359 (1981); **14**, 2345 (1981).

[8] B. Lewandowski, J. Ganz, H. Hotop, and M.-W. Ruf, J. Phys. B **14**, L803 (1981).

[9] D. M. P. Holland, K. Codling, and J. B. West, J. Phys. B **15**, 1473 (1982).

[10] S. L. Carter and H. P. Kelly, Phys. Rev. A **24**, 170 (1981).

[11] F. J. Wuilleumier, Ann. Phys. **4**, 231 (1982).

[12] V. Schmidt, in *X-Ray and Inner-Shell Processes,* edited by T. A. Carlson, M. O. Krause, and S. T. Manson, AIP Conf. Proc. No. **215** (American Institute of Physics, New York, 1990), p. 559.

[13] P. Lablanquie, in *Electronic and Atomic Collisions,* edited by W. R. McGillivray, I. E. McCarthy, and M. C. Standage (Adam-Hilger, New York, 1992), p. 507.

[14] V. Schmidt, Rep. Prog. Phys. **55**, 1431 (1992).

[15] P. Lablanquie, J. H. D. Eland, I. Nenner, P. Morin, J. Delwiche, and M. Hubin-Franskin, Phys. Rev. Lett. **58**, 992 (1987).

[16] H. Kossman, V. Schmidt, and T. Andersen, Phys. Rev. Lett. **60**, 1266 (1988).

[17] P. Lablanquie, K. Ito, P. Morin, I. Nenner, and J. H. D. Eland, Z. Phys. D **16**, 77 (1990).

[18] R. I. Hall, L. Avaldi, G. Dawber, M. Zubek, K. Ellis, and G. C. King, J. Phys. B **24**, 115 (1991).

[19] R. Wehlitz, F. Heiser, O. Hemmers, B. Langer, A. Menzel, and U. Becker, Phys. Rev. Lett. **67**, 3764 (1991).

[20] B. Krässig and V. Schmidt, J. Phys. B **25**, L327 (1992).

[21] R. I. Hall, A. McConkey, L. Avaldi, K. Ellis, M. A. McDonald, G. Dawber, and G. C. King, J. Phys. B **25**, 1195 (1992).

[22] R. I. Hall, G. Dawber, A. McConkey, M. A. McDonald, and G. C. King, Z. Phys. D **23**, 377 (1992).

[23] R. I. Hall, A. McConkey, K. Ellis, G. Dawber, M. A. MacDonald, and G. C. King, J. Phys. B **25**, 799 (1992).

[24] J. C. Levin, D. W. Lindle, N. Keller, R. D. Miller, Y. Azuma, N. Berrah Mansour, H. G. Berry, and I. A. Sellin, Phys. Rev. Lett. **67**, 968 (1991).

[25] J. C. Levin, I. A. Sellin, B. M. Johnson, D. W. Lindle, R. D. Miller, N. Berrah, Y. Azuma, H. G. Berry, and D. H. Lee, Phys. Rev. A **47**, R16 (1993).

[26] N. Berrah, F. Heiser, R. Wehlitz, J. Levin, S. B. Whitfield, J. Viefhaus, I. A. Sellin, and U. Becker, Phys. Rev. A **48**, R1733 (1993).

[27] R. J. Bartlett, P. J. Walsh, Z. X. He, Y. Chung, E.-M. Lee, and J. A. R. Samson, Phys. Rev. **46**, 5574 (1992), and references therein.

[28] G. C. Angel and J. A. R. Samson, Phys. Rev. A **38**, 5578 (1988).

[29] G. C. Angel and J. A. R. Samson, Phys. Rev. A **42**, 1307 (1990); **42**, 5328 (1990).

[30] J. Mazeau, P. Selles, D. Waymel, and A. Huetz A., Phys. Rev. Lett. **67**, 820 (1991).

[31] A. Huetz, P. Selles, D. Waymel, and J. Mazeau, J. Phys. B **24**, 1917 (1991).

[32] A. Huetz, P. Selles, D. Waymel, and J. Mazeau, in *Correlations and Polarization in Electronic and Atomic Collisions and (e,2e) Reactions,* edited by P. J. O. Teubner and E. Weigold, IOP Conf. Proc. No. 122 (Institute of Physics and Physical Society, London, 1992), pp. 213–222.

[33] A. Huetz, P. Selles, D. Waymel, L. Andric, and J. Mazeau, in *Proceedings of the NATO Advanced Research Workshop on (e,2e) and Related Processes,* edited by C. T. Whelan, H. R. J. Walters, A. Lahmam-Bennani, and H. Ehrhardt (Kluwer, Dordrecht, 1993), p. 297.

[34] O. Schwarzkopf, B. Krässig, J. Elmiger, and V. Schmidt, Phys. Rev. Lett. **70**, 3008 (1993).

[35] A. Huetz, P. Lablanquie, L. Andric, P. Selles, and J. Mazeau, J. Phys. B **27**, L13 (1994).

[36] T. Ishihara, K. Hino, and J. H. McGuire, Phys. Rev. A **44**, R6980 (1991).

[37] J. A. R. Samson, C. Greene, and R. J. Bartlett, Phys. Rev. Lett. **71**, 201 (1993).

[38] K. Hino, T. Ishihara, F. Shimizu, N. Toshima, and J. H. McGuire, Phys. Rev. A **48**, 1271 (1993).

[39] D. Proulx and R. Shakeshaft, Phys. Rev. A **48**, R875 (1993).

[40] L. R. Andersson and J. Burgdörfer, Phys. Rev. Lett. **71**, 50 (1993).

[41] K. Hino, P. M. Bergstrom, and J. H. Macek, Phys. Rev. Lett. **72**, 1620 (1994).

[42] E. Von Raven, M. Meyer, M. Pahler, and B. Sonntag, J.

Electron. Spectrosc. Relat. Phenom. **52**, 677 (1990).
[43] M. O. Krause, M. L. Vestal, W. M. Johnston, and T. A. Carlson, Phys. Rev. A **133**, 385 (1964).
[44] T. A. Carlson and M. O. Krause, Phys. Rev. Lett. **14**, 390 (1965).
[45] T. A. Carlson and M. O. Krause, Phys. Rev. Lett. **17**, 1079 (1966).
[46] T. Mukoyama, T. Tonuma, A. Yaghishita, H. Shibata, T. Koizumi, T. Matsuo, K. Shima, and J. Tawara, J. Phys. B **20**, 4453 (1987).
[47] D. W. Lindle, P. A. Heimann, T. A. Ferrett, M. N. Piancastelli, and D. A. Shirley, Phys. Rev. A **35**, 4605 (1987).
[48] P. A. Heimann, D. W. Lindle, T. A. Ferrett, S. H. Liu, L. J. Medhurst, M. N. Piancastelli, D. A. Shirley, U. Becker, H. G. Kerkhoff, B. Langer, D. Szostak, and R. Wehlitz, J. Phys. B **20**, 5005 (1987).
[49] T. A. Carlson, D. R. Mullins, C. E. Beall, B. W. Yates, J. W. Taylor, D. W. Lindle, B. P. Pullen, and F. A. Grimm, Phys. Rev. Lett. **60**, 1382 (1988).
[50] T. Hayaishi, E. Murakami, A. Y. Yagishita, F. Koike, Y. Morioka, and J. E. Hansen, J. Phys. B **21**, 3203 (1988).
[51] H. Aksela, S. Aksela, H. Pulkkinen, and A. Yaghishita, Phys. Rev. A **40**, 6275 (1989).
[52] U. Becker, T. Prescher, E. Schmidt, B. Sonntag, and H.-E. Wetzel, Phys. Rev. A **33**, 3891 (1989).
[53] U. Becker, D. Szostak, M. Kupsch, H. G. Kerkhoff, B. Langer, and R. Wehlitz, J. Phys. B **22**, 749 (1989).
[54] H. Aksela, S. Aksela, G. M. Brancroft, K. H. Tan, and H. Pulkkinen, Phys. Rev. A **33**, 3867 (1989).
[55] B. Kämmerling, B. Krässig, and V. Schmidt, J. Phys. B **23**, 4487 (1990).
[56] T. Hayaishi, A. Y. Yagishita, E. Murakami, E. Shigemasa, Y. Morioka, and T. Sasaki, J. Phys. B **23**, 1633 (1990).
[57] T. Hayaishi, A. Y. Yagishita, E. Shigemasa, E. Murakami, and Y. Morioka, J. Phys. B **23**, 4431 (1990).
[58] P. Lablanquie and P. Morin, J. Phys. B **24**, 4349 (1991).
[59] T. Hayaishi, E. Murakami, Y. Morioka, H. Aksela, S. Aksela, E. Shigemasa, and A. Y. Yagishita, Phys. Rev. A **44**, 2771 (1991).
[60] K. Ueda, E. Shigemasa, Y. Sato, A. Y. Yagishita, M. Ukai, H. Maezawa, T. Hayaishi, and T. Sasaki, J. Phys. B **24**, 605 (1991).
[61] Y. Sato, Y. Hayaishi, Y. Itikawa, Y. Itoh, J. Murakami, T. Nagata, T. Sasaki, B. Sonntag, A. Yagishita, and M. Yoshino, J. Phys. B **18**, 225 (1985).
[62] T. Nagata, J. B. West, T. Hayaishi, Y. Itikawa, Y. Itoh, T. Koizumi, J. Murakami, Y. Sato, H. Shibata, A. Yagisgita, and M. Yoshino, J. Phys. B **19**, 1281 (1986).
[63] T. Koizumi, T. Hayaishi, Y. Itakawa, T. Nagata, Y. Sato, and A. Yagishita, J. Phys. B **20**, 5393 (1987).
[64] A. Yagishita, S. Aksela, T. Prescher, M. Meyer, M. Richter, E. von Raven, and B. Sonntag, J. Phys. B **21**, 945 (1988).
[65] T. Nagata, Y. Itoh, T. Hayaishi, Y. Itakawa, T. Koizumi, T. Matsuo, Y. Sato, E. Shigemasa, A. Yagishita, and Y. Yoshino, J. Phys. B **22**, 3865 (1989).
[66] C. Dzionk, W. Fiedler, M. von Lucke, and P. Zimmermann, Phys. Rev. Lett. **62**, 878 (1989).
[67] M. Y. Adam, L. Hellner, G. Dujardin, S. Svensson, P. Martin, and F. Combet Farnoux, J. Phys. B **22**, 2141 (1989).
[68] F. Combet Farnoux, G. Dujardin, L. Hellner, and M. Y. Adam, in *X-Ray and Inner-Shell Processes* (Ref. [12]), p. 281.
[69] T. Koizumi, T. Hayaishi, Y. Itikawa, Y. Itoh, T. Matsuo, T. Nagata, Y. Sato, E. Shigemasa, A. Yagishita, and M. Yoshino, J. Phys. B **23**, 403 (1990).
[70] T. Matsuo, T. Hayaishi, Y. Itoh, T. Koizumi, T. Nagata, Y. Sato, E. Shigemasa, A. Yagishita, M. Yoshino, and Y. Itakawa, J. Phys. B **25**, 121 (1992).
[71] B. Sonntag and P. Zimmermann, Rep. Prog. Phys. **55**, 911 (1992).
[72] U. Becker and D. A. Shirley, Phys. Scr. T **31**, 56 (1990).
[73] L. Journel, B. Rouvellou, D. Cubaynes, J.-M. Bizau, F. J. Wuilleumier, M. Richter, P. Sladeczek, K.-H. Selbmann, P. Zimmermann, and H. Bergeron, J. Physique IV Colloq. **3**, C6-217 (1993).
[74] Ch. E. Moore, *Atomic Energy Levels I* (US Government Printing Office, Washington, D.C. 1949).
[75] H. W. Wolff, K. Radler, B. Sonntag, and R. Haensel, Z. Phys. **257**, 353 (1972).
[76] K. Codling, J. R. Hamley, and J. B. West, J. Phys. B **10**, 2797 (1977).
[77] V. Schmidt, Phys. Lett. **45A**, 63 (1973).
[78] D. Cubaynes, J. M. Bizau, F. J. Wuilleumier, B. Carré, and F. Gounand, Phys. Rev. Lett. **63**, 2460 (1989).
[79] F. J. Wuilleumier and M. O. Krause, Phys. Rev. A **10**, 242 (1974).
[80] Z. W. Liu and J. C. Liu, Bull. Am. Phys. Soc. **38**, 1150 (1993).
[81] M. Richter, J. M. Bizau, D. Cubaynes, T. Menzel, F. J. Wuilleumier, and B. Carré, Europhys. Lett. **12**, 35 (1990).
[82] E. Breuckmann, B. Breuckmann, W. Mehlhorn, and W. Schmitz, J. Phys. B **10**, 3135 (1977).
[83] L. VoKy (private communication).
[84] R. E. LaVilla, G. Mehlman, and E. B. Saloman, J. Phys. B **14**, L1 (1981).
[85] T. N. Chang and R. T. Poe, Phys. Rev. A **12**, 1432 (1975).
[86] P. A. Heiman, C. M. Truesdale, H. G. Kerkhoff, D. W. Lindle, T. A. Ferrett, C. C. Bahr, W. D. Brewer, U. Becker, and D. A. Shirley, Phys. Rev. A **31**, 2260 (1985).
[87] M. O. Krause, S. B. Whitfield, C. D. Caldwell, J.-Z. Wu, P. van der Meulen, C. A. de Lange, and R. W. C. Hansen, J. Electron Spectrosc. Relat. Phenom. **58**, 79 (1992).
[88] J.-M. Bizau and F. J. Wuilleumier, J. Electron Spectrosc. Relat. Phenom. (to be published).
[89] F. J. Wuilleumier, L. Journel, B. Rouvellou, D. Cubaynes, J.-M. Bizau, Z. Liu, J. Liu, M. Richter, P. Sladeczek, K.-H. Selbman, and P. Zimmermann, Phys. Rev. Lett. (to be published).